

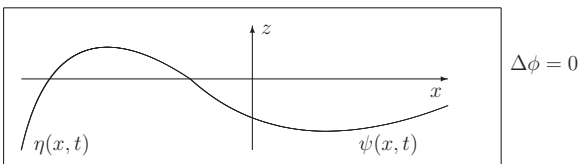
Probability Distribution Functions of Freak Waves: Nonlinear Versus Linear Model

By Alexander I. Dyachenko, Dmitriy I. Kachulin, and Vladimir E. Zakharov

Presented are the results of numerical experiments on calculation of probability distribution functions (PDFs) for surface elevations of water waves arising during the evolution of statistically homogeneous wave field. Extreme waves or freak waves are an integral part of ocean waving, and PDFs are compared both for nonlinear and linear models. Obviously, linear model demonstrates the Rayleigh distribution of surface elevations while PDFs for nonlinear equation have tails for large elevations similar to Rayleigh distribution, but with much larger σ .

1. Introduction

No doubts that estimation of probability of extreme waves, or freak wave, appearing at the surface of ocean has practical meaning. They are a native part of the surface wave dynamics in the open seas, and among different mechanisms of this phenomenon, linear dispersion and modulational instability are generally recognized. We study these two mechanisms for the classical 1-D water wave Hamiltonian system:



Address for correspondence: Alexander I. Dyachenko, Landau Institute for Theoretical Physics - 142432, Chernogolovka, Russia, e-mail: alexd@itp.ac.ru

DOI: 10.1111/sapm.12116

STUDIES IN APPLIED MATHEMATICS 137:189–198

© 2016 Wiley Periodicals, Inc., A Wiley Company

picture with the Hamiltonian

$$H = \frac{1}{2} \int dx \int_{-\infty}^{\eta} |\nabla\phi|^2 dz + \frac{g}{2} \int \eta^2 dx,$$

where $\phi(x, z, t)$ is the potential of the fluid, g is gravity acceleration, and $\eta(x, t)$ is surface profile. As it was shown in [1] the Hamiltonian variables are $\eta(x, t)$ and $\psi(x, t) = \phi(x, \eta(x, t), t)$

$$\frac{\partial\psi}{\partial t} = -\frac{\delta H}{\delta\eta} \quad \frac{\partial\eta}{\partial t} = \frac{\delta H}{\delta\psi}.$$

In the system there is natural small parameter, steepness (slope $\sim \eta'_x$) of the waves μ . The Hamiltonian can be expanded as infinite series on this small parameter (see [1, 2]):

$$\begin{aligned} H &= H_2 + H_3 + H_4 + \dots \\ H_2 &= \frac{1}{2} \int (g\eta^2 + \psi \hat{k} \psi) dx, \\ H_3 &= -\frac{1}{2} \int \{(\hat{k}\psi)^2 - (\psi_x)^2\} \eta dx, \\ H_4 &= \frac{1}{2} \int \{\psi_{xx} \eta^2 \hat{k} \psi + \psi \hat{k} (\eta \hat{k} (\eta \hat{k} \psi))\} dx, \end{aligned} \quad (1)$$

where \hat{k} corresponds to the multiplication by $|k|$ in Fourier space. This truncated Hamiltonian is enough for gravity waves of moderate amplitudes and cannot be reduced. The nonlinear equation we use to calculate probability distribution functions (PDFs) is based, but does not coincide with, on truncated Hamiltonian. The equation is obtained using canonical transformation applied to (1) and will be discussed in the next section.

The linear model has the only quadratic part (H_2) of the Hamiltonian (1). PDF for homogeneous initial conditions is nothing but normal Gaussian distribution for surface elevation, or Rayleigh distribution for absolute values of elevation. Nonlinear waves present something very different.

The above leads to the problems of great practical importance: Could a captain estimate a probability to face an extreme wave or freak wave within the next few ours? What information about spectrum of sea waving is enough to make the estimation?

Questions such as these have been posed in many articles dealing with statistics of extreme (freak or rogue) waves. All physical mechanisms of freak waves arising are demonstrated in [3] which include spatial focusing, dispersive focusing, and nonlinear focusing. We focus on the last two. We recall that for the linear model of water waves statistic of amplitudes of waves is Gaussian. For nonlinear models, deviation from Gaussian statistics was always observed [4, 5]. Oceanic waves display sharper and narrower

crests with more rounded trough. It leads to asymmetry between crests and troughs. Skewness of wave amplitude distribution is not equal to zero. This asymmetry was studied in details in [6].

In our article we eliminated nonresonant three-waves interactions (no skewness) and applied proper canonical transformation to the Hamiltonian of the nonlinear water waves equation. The nonlinear equation obtained is discussed below. Then we consider and compare statistics providing both linear and nonlinear models.

2. Compact equation for water waves

We derived a compact equation (and new Hamiltonian) beginning with the following Hamiltonian:

$$H = \frac{1}{2} \int (g\eta^2 + \psi \hat{k} \psi) dx - \frac{1}{2} \int \{(\hat{k}\psi)^2 - (\psi_x)^2\} \eta dx + \frac{1}{2} \int \{\psi_{xx} \eta^2 \hat{k} \psi + \psi \hat{k} (\eta \hat{k} (\eta \hat{k} \psi))\} dx. \quad (2)$$

For our purpose, Hamiltonian expanded up to the fourth order was sufficient. However, before doing simulations, we applied canonical transformation to the Hamiltonian (2) to make the resulting equation much more simple. This canonical transformation is described in detail in [7, 8]. Following is our brief explanation of the idea of the transformation:

- First instead of η and ψ normal canonical variable a_k is introduced

$$\eta_k = \sqrt{\frac{\omega_k}{2g}} (a_k + a_{-k}^*) \quad \psi_k = -i \sqrt{\frac{g}{2\omega_k}} (a_k - a_{-k}^*) \quad \omega_k = \sqrt{gk}.$$

- Canonical transformation from a_k to b_k is chosen to cancel all nonresonant terms in the Hamiltonian, both cubic and fourth order.
- The only term (that corresponds four wave interaction $2 \leftrightarrow 2$) acquires a simple form.

This transformation explicitly uses vanishing of four-wave interaction on the resonant manifold with one negative k , see [9]:

$$\begin{aligned} k + k_1 &= k_2 + k_3, \\ \omega_k + \omega_{k_1} &= \omega_{k_2} + \omega_{k_3}, \end{aligned} \quad (3)$$

with nontrivial solution:

$$\begin{aligned} k &= a(1 + \zeta)^2, \\ k_1 &= a(1 + \zeta)^2 \zeta^2, \end{aligned}$$

$$\begin{aligned} k_2 &= -a\zeta^2, \\ k_3 &= a(1 + \zeta + \zeta^2)^2. \end{aligned} \quad (4)$$

Here $0 < \zeta < 1$ and $a > 0$. This property of four wave interaction coefficient allows for the consideration of surface waves moving in one direction. This coefficient is not equal zero on the trivial resonant manifold only:

$$\begin{aligned} k = k_2, k_1 = k_3 & \quad \omega_k = \omega_{k_2}, \omega_{k_1} = \omega_{k_3}, \\ \text{or} \\ k = k_3, k_1 = k_2 & \quad \omega_k = \omega_{k_3}, \omega_{k_1} = \omega_{k_2}. \end{aligned} \quad (5)$$

For this variable $b(x, t)$ Hamiltonian (2) acquires nice and elegant form:

$$\mathcal{H} = \int b^* \hat{\omega}_k b dx + \frac{1}{2} \int \left| \frac{\partial b}{\partial x} \right|^2 \left[\frac{i}{2} \left(b \frac{\partial b^*}{\partial x} - b^* \frac{\partial b}{\partial x} \right) - \hat{k} |b|^2 \right] dx. \quad (6)$$

Corresponding equation of motion is the following:

$$\begin{aligned} i \frac{\partial b}{\partial t} &= \hat{\omega}_k b + \frac{i}{4} \hat{P}^+ \left[b^* \frac{\partial}{\partial x} (b'^2) - \frac{\partial}{\partial x} (b^* \frac{\partial}{\partial x} b^2) \right] \\ &\quad - \frac{1}{2} \hat{P}^+ \left[b \cdot \hat{k} (|b'|^2) - \frac{\partial}{\partial x} (b' \hat{k} (|b|^2)) \right], \end{aligned} \quad (7)$$

where $b' = \frac{\partial b}{\partial x}$, $\hat{\omega}_k$ is just \sqrt{gk} in k -space.

Projection operator \hat{P}^+ provides vanishing four-wave interaction on the resonant manifold (4). In the Fourier-space its eigenvalue is step-function:

$$P_k^+ = \theta(k) = \begin{cases} 1, & k > 0; \\ 0, & k \leq 0. \end{cases}$$

Motion equation in k -space is the following:

$$i \frac{\partial b_k}{\partial t} = \omega_k b_k + \theta(k) \int \tilde{T}_{kk_1}^{k_2 k_3} b_{k_1}^* b_{k_2} b_{k_3} \delta_{k+k_1-k_2-k_3} dk_1 dk_2 dk_3. \quad (8)$$

Note that $b(x, t)$ is an analytic function of x in the upper half-plane, because it has only positive Fourier harmonics.

Transformation from $b(x, t)$ to physical variables $\eta(x, t)$ and $\psi(x, t)$ can be recovered from canonical transformation [10]. Following is this transformation up to the second order:

$$\begin{aligned}
\eta(x) &= \frac{1}{\sqrt{2}g^{\frac{1}{4}}}(\hat{k}^{\frac{1}{4}}b(x) + \hat{k}^{\frac{1}{4}}b(x)^*) + \frac{\hat{k}}{4\sqrt{g}}[\hat{k}^{\frac{1}{4}}b(x) - \hat{k}^{\frac{1}{4}}b^*(x)]^2, \\
\psi(x) &= -i\frac{g^{\frac{1}{4}}}{\sqrt{2}}(\hat{k}^{-\frac{1}{4}}b(x) - \hat{k}^{-\frac{1}{4}}b(x)^*) + \frac{i}{2}[\hat{k}^{\frac{1}{4}}b^*(x)\hat{k}^{\frac{3}{4}}b^*(x) - \hat{k}^{\frac{1}{4}}b(x)\hat{k}^{\frac{3}{4}}b(x)] \\
&\quad + \frac{1}{2}\hat{H}[\hat{k}^{\frac{1}{4}}b(x)\hat{k}^{\frac{3}{4}}b^*(x) + \hat{k}^{\frac{1}{4}}b^*(x)\hat{k}^{\frac{3}{4}}b(x)]. \tag{9}
\end{aligned}$$

Here \hat{H} is Hilbert transformation with eigenvalue $i \text{sign}(k)$.

3. How we calculate PDFs

Following is the idea of the numerical experiment:

- In the framework of the nonlinear equation (7), stationary turbulent state “is prepared.” Obviously, pumping and damping must be included in the equation.
- When stationary state is reached, one can calculate PDF for *this nonlinear equation*
- Subsequently, one can turn off nonlinear term along with pumping and damping in Equation (7) and continue a parallel RUN calculating PDF for *that linear equation*.

Both of these RUNS have practically the same energy and average steepness.

Following is the equation with added pumping and damping in k -space:

$$i \left(\frac{\partial b_k}{\partial t} + \Gamma_p(k)b_k - \Gamma_d(k)b_k \right) = \omega_k b_k + \int \tilde{T}_{kk_1}^{k_2 k_3} b_{k_1}^* b_{k_2} b_{k_3} \delta_{k+k_1-k_2-k_3} dk_1 dk_2 dk_3, \tag{10}$$

simulations were performed in the periodic domain $L = 2\pi$.

Here pumping coefficient $\Gamma_p(k)$ is the following:

$$\Gamma_p(k) = \begin{cases} \gamma_{max} e^{-\frac{(k-k_0)^2}{2\sigma_\gamma^2}} & \text{if } |k - k_0| \leq 5 \\ 0 & \text{if } |k - k_0| > 5 \end{cases}$$

with $k_0 = 100$, $\sigma_\gamma = 5$. Coefficient of pumping γ_{max} was equal to 10^{-3} or less.

Damping coefficient $\Gamma_d(k)$ was switched on if the values of b_k for $k \sim k_{max}$ were larger than roundoff errors. Namely, value of b_C , which is

$$b_C = \frac{1}{10} \sum_{i=9}^0 |b_{k_{max}-i}|,$$

controls the damping in the following way:

$$\Gamma_d(k) = \begin{cases} \alpha k^2 & \text{if } b_C \text{ is 10 times greater than roundoff errors} \\ 0 & \text{in the other case} \end{cases}$$

with $\alpha = 0.9/\tau k_{max}^2$ (recall that all k are positive in the compact equation).

To reach a stationary turbulent state, one can start from different initial conditions. We started with the initial conditions for (10) as a perturbed monochromatic wave:

$$b(x, t) = b_0 e^{ik_0 x} + \text{perturbation}$$

with $b_0 = 2.2 \times 10^{-4}$, $k_0 = 100$ corresponding to the maximal steepness $\mu \sim 0.1$. This perturbation undergoes modulational instability and after some time, ~ 1200 , turbulent state (statistically homogeneous) was reached and we began to collect data for PDFs. Starting from this time, we have performed simulation for:

- Equation (10)
- linear equation $i \frac{\partial b_k}{\partial t} = \omega_k b_k$

We were interested in distribution of values of $Re\{b(x, t)\} = r(x, t)$ and $|b|^2$. So at some times t_n data were collected into unnormalized UPDF in the following way:

$$N = r(x_i, t_n)/\delta b, \quad UPDF(N\delta b) = UPDF(N\delta b) + 1.$$

Here δb is discrete step for PDF. At the very end of data collection UPDF was normalized.

For a linear equation, one can expect normal distribution for $r(x, t)$ and Rayleigh distribution for $|b|$:

$$PDF(r) = \frac{1}{\sigma\sqrt{2\pi}} e^{-\frac{r^2}{2\sigma^2}},$$

$$PDF(|b|) = \frac{|b|}{\sigma^2} e^{-\frac{|b|^2}{2\sigma^2}},$$

with some dispersion σ .

Note: normalization was done so that for linear equations σ was equal to 1.

It is obvious that PDF of $r(x, t)$ is even function (symmetric) of r ,

$$PDF(r) = PDF(-r).$$

It is the consequence of the absence of quadratic terms (three-wave interaction) in (10) while PDF of real surface elevation $\eta(x, t)$ is not symmetric. This is because troughs have less amplitudes than the crests.

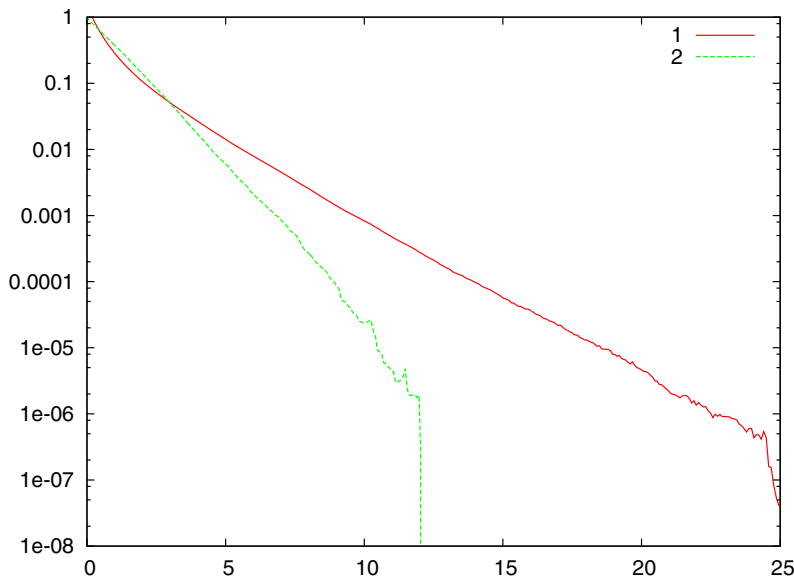


Figure 1. $\text{Log}(\text{PDF}(|b|)/|b|)$ as function of $|b|^2$ is shown for $\mu \simeq 0.1$. 1 (solid line) – nonlinear equation, 2 (dashed line) – linear equation. Extreme waves start at $|b|^2 \simeq 9$.

It is convenient to plot $\text{PDF}(|b|)/|b|$ in logarithmic scale and as a function of $|b|^2$. For this case, Rayleigh distribution looks like a straight line with the slope defined by σ :

$$\text{Log}(\text{PDF}(|b|)/|b|) \simeq -\frac{|b|^2}{2\sigma^2}.$$

For the nonlinear equation (10) PDF also has Rayleigh tail—straight lines for large $|b|^2$, while the small $|b|^2$ are different. This is clearly portrayed in Figure 1. The level of turbulence here is moderate averaged steepness $\mu \sim 0.1$.

It should be mentioned that extreme wave is the wave with the amplitude about three times larger than the average wave amplitude. It corresponds to $|b|^2 \simeq 9$ in Figure 1.

For further explanation, consult the following:

<http://alex.d.itp.ac.ru/SAPM/PDF.avi> for dynamic (animation) of collection of extreme waves statistics.

<http://alex.d.itp.ac.ru/SAPM/PDFeta.avi> for distribution of η instead of $|b|$ for the same data (the same RUN) which clearly expresses skewness while distribution of $\text{Re}\{b(x, t)\}$ has no skewness at all: <http://alex.d.itp.ac.ru/SAPM/PDFReb.avi>.

<http://alex.d.itp.ac.ru/SAPM/Spectrum.avi> and <http://alex.d.itp.ac.ru/SAPM/SpectrumNOLOG.avi> for evolution of spectrum of $|b_k|$.

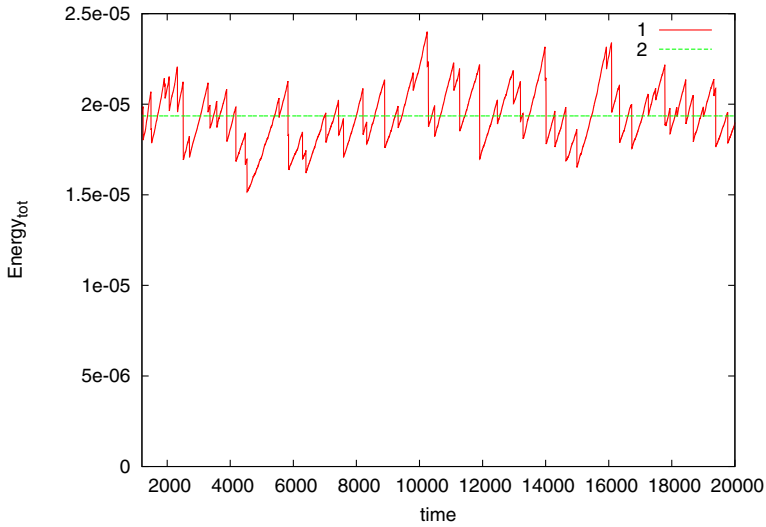


Figure 2. (Solid line-1) – energy of turbulent states for nonlinear equation, (dashed line-2) – linear equation -2.

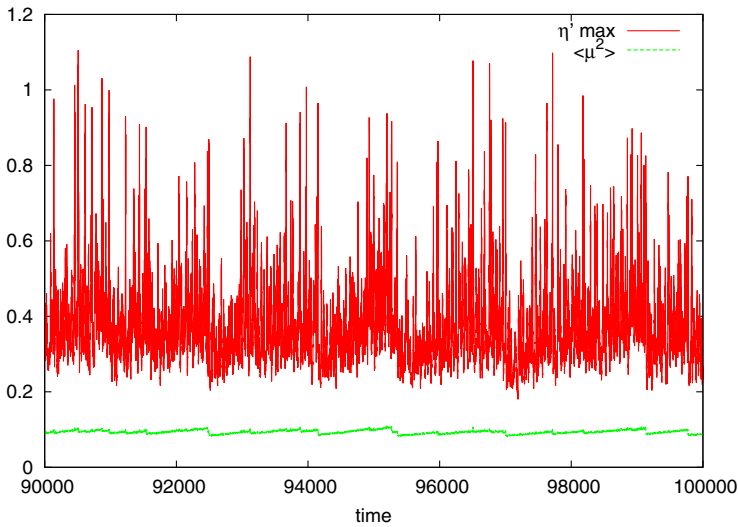


Figure 3. Averaged steepness (dashed line) and maximal value of wave slope (solid line) are shown for nonlinear equation.

Although average squared elevation is the same for both linear and nonlinear cases (the energy of the system), σ^2 estimated exclusively by tail for the nonlinear equation is two times larger than for linear equation. Probability to face extreme wave (with $|b|^2 > 3$) is almost 100 times larger than in the linear case.

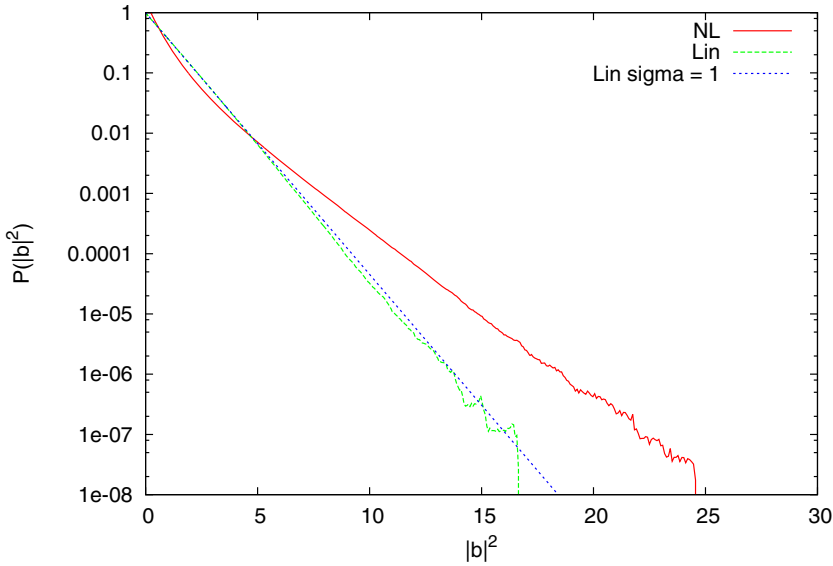


Figure 4. $\text{Log}(\text{PDF}(|b|)/|b|)$ as function of $|b|^2$ is shown for $\mu \simeq 0.08$. 1 (solid line) – nonlinear equation, 2 (dashed line) – linear equation, 3 (dotted line) – Rayleigh distribution with $\sigma = 1$. Extreme waves start at $|b|^2 \simeq 9$.

Evolution of energy for both linear and nonlinear cases is shown in Figure 2. Notice the stationary levels of turbulence are the same. Figure 3 shows the value of maximal steepness (over x-domain) along with the average steepness. PDFs calculated for nonlinear equations for smaller levels of steepness and energy also have Gaussian tails, but σ is closer to 1. See Figure 4.

4. Conclusion

We have shown numerically that the PDF of surface elevations has Gaussian tail similar to linear equation. The reason may be due to the fact of “almost” integrability of Equation (8). It is not integrable only in the next or sixth order as shown in [11]. Such trivial resonance manifold as (5) could be responsible for the “almost” Rayleigh distribution of surface elevations in this nonlinear equation. Providing steepness and energy were the same for both linear and nonlinear cases, we observed σ_{NL} calculated exclusively by tails in the framework of nonlinear equation much greater than σ_L calculated for linear model:

$$\sigma_{NL} = \alpha \times \sigma_L,$$

$\alpha > 1$ and depends somehow on average steepness.

It should be emphasized that when calculating PDF for real surface elevation $\eta(x, t)$ from (2) (like in the article [12]) one get nonsymmetric, non-Gaussian tails for $\eta(x, t)$. It is why we call $Re\{b(x, t)\} = r(x, t)$ “surface elevation” in quotation marks.

Acknowledgments

Numerical part of this work including linear and nonlinear simulation of water waves and calculating probability distribution functions of freak waves was supported by the Grant “Wave turbulence: theory, numerical simulation, experiment” #14-22-00174 of Russian Science Foundation. Analytical part of the article was supported by Grant of NSF 1130450.

Numerical simulation was performed at the Informational Computational Center of the Novosibirsk State University.

References

1. V. E. ZAKHAROV, *J. Appl. Mech. Tech. Phys.* 9(2):190 (1968).
2. D. E. CRAWFORD, H. G. YUEN, and P. G. SAFFMAN, *Wave Motion* 2:1 (1980).
3. K. DYSTHE, H. E. KROGSTAD, and P. MÜLLER, *Annu. Rev. Fluid Mech.* 40:287 (2008).
4. M. ONORATO et al., *Phys. Fluids* 17:078101 (2005).
5. F. FEDELE and F. ARENA, *Phys. Fluids* 17:026601 (2005).
6. F. FEDELE and M. TAYFUN, *J. Fluid Mech.* 620:221 (2009).
7. A. I. DYACHENKO and V. E. ZAKHAROV, Compact equation for gravity waves on deep water, *JETP Lett.* 93(12):701 (2011).
8. A. I. DYACHENKO and V. E. ZAKHAROV, A dynamical equation for water waves in one horizontal dimension, *Eur. J. Mech. B* 32:17 (2012).
9. A. I. DYACHENKO and V. E. ZAKHAROV, *Phys. Lett. A.* 190:144 (1994).
10. A. I. DYACHENKO, D. I. KACHULIN, and V. E. ZAKHAROV, Freak-waves: Compact equation vs fully nonlinear one, in *Extreme Ocean Waves* (2nd ed.) (E. Pelinovsky and C. Harif, Eds.), pp. 23–44, Springer International Publishing Switzerland, 2015.
11. A. I. DYACHENKO, D. I. KACHULIN, and V. E. ZAKHAROV, *JETP Lett.* 98(1):43 (2013).
12. M. ONORATO, L. CAVALERI et al., *JFM* 627:235 (2009).

NOVOSIBIRSK STATE UNIVERSITY, 630090, NOVOSIBIRSK-90, RUSSIA

LANDAU INSTITUTE FOR THEORETICAL PHYSICS, 142432, CHERNOGOLOVKA, RUSSIA

DEPARTMENT OF MATHEMATICS UNIVERSITY OF ARIZONA, TUCSON, AZ, 857201, USA

PHYSICAL INSTITUTE OF RAS, LENINSKIY PROSPEKT, 53, MOSCOW, 119991, RUSSIA

(Received August 14, 2015)

Copyright of Studies in Applied Mathematics is the property of Wiley-Blackwell and its content may not be copied or emailed to multiple sites or posted to a listserv without the copyright holder's express written permission. However, users may print, download, or email articles for individual use.